

## Selection of lamellar thickness in polymer crystal growth: A rate-theory model

David M. Sadler

*H. H. Wills Physical Laboratory, University of Bristol, Royal Fort, Bristol BS8 1TL, Avon, United Kingdom*

George H. Gilmer

*AT&T Bell Laboratories, Murray Hill, New Jersey 07974*

(Received 3 June 1988)

We discuss a rate-theory model of polymer crystallization that exhibits many of the morphological and kinetic features observed in the laboratory. The interplay between the growth of the lamellar crystals in directions along the molecular direction and at right angles to it is discussed, together with some of the implications for the temperature dependence of the thickness of the crystals. We examine in some detail the hypothesis that the growth process selects the thickness that maximizes the rate of advance of the lamellar edge.

### INTRODUCTION

A new theory of chain folding during polymer crystallization is being developed which applies to systems with a range of step(niche)-free energies. Previous theories<sup>1-5</sup> require step-free energies,  $\sigma_n$ , which are of the order of  $10kT$ , whereas the morphologies observed for many crystals show that steps are much more numerous than this value of  $\sigma_n$  would imply.<sup>6-10</sup> Computer simulation studies of systems with rough growth surfaces led to a model that included a mechanism for pinning a crystallized segment of a polymer molecule at a fixed length.<sup>11</sup> A very simple two-dimensional (2D) rate-theory model based on a single row of stems demonstrates the principal effects.<sup>11</sup> A stem is a section of chain in the crystal that traverses the lamella.

The main purpose of this paper is to understand precisely what determines the value of the lamellar thickness  $l$ . In order to do this, the equation for the growth of the row model is rewritten in terms of two factors which can be identified with physical processes. One is the probability of surmounting a barrier, and the other represents the growth rate once such a barrier has been reached. We then test the results of the analysis against a criterion for a kinetic model: that the thickness which results corresponds to the fastest mode of growth. In doing so the important distinction is made between ensembles of crystals of uniform thickness, and those where fluctuations in  $l$  values are allowed within individual crystals.

### REVIEW OF THE MODELS

First, we discuss various models of polymer crystallization and their implications for the lamellar thickness. The rate-theory row model and previous "nucleation" theories explain the almost universal chain-folded (lamellar) habit<sup>12,13</sup> by supposing that the growth kinetics are faster for thin crystals, and therefore that thin crystals dominate in the ensemble. The average crystal thickness  $l$  is therefore only slightly larger than the thickness  $l_m$  corresponding to thermodynamic stability; i.e.,

$l = l_m + \delta l$ , where  $\delta l$  is a small fraction of  $l_m$ . The value of  $l_m$  is calculated by equating the surface excess free energy with the bulk free energy of crystallization, which gives  $l_m \propto \Delta T^{-1}$ , where  $\Delta T$  is the undercooling relative to the bulk melting point  $T_M^0$ . ( $T_M^0$  is the limit of the lamellar melting temperatures as  $l$  approaches infinity.) Since the  $\Delta T$  dependence of  $l$  is dominated by  $l_m$ ,  $l \propto \Delta T^{-1}$ , which is one of the principal observations for most polymer crystallization systems.

The rate-theory model discussed here differs from the nucleation theories as to the identity of the high free-energy step that must be surmounted for growth to proceed. Nucleation theories identify a barrier corresponding to the creation of a step on the growth face with free energy  $\sigma_n$ , an essential feature being that its magnitude increases linearly with  $l$ . One of us has argued<sup>6-10</sup> that the morphology is not consistent with this assumption, since the large step densities implied by curved lamellar edges do not enhance the growth rate by the required amount. Even in the case of relatively straight edges, it has been shown that a plentiful supply of reentrant corners has a small effect on the growth rate.<sup>9</sup>

The new models exhibit a different barrier to the growth process, a state with low entropy, and the free energy of this state also increases in magnitude with  $l$ . The presence of this low-entropy barrier is a consequence of two factors: (a) the tendency of the growth faces of the lamellae to assume a rounded shape, in vertical cross section, with relatively short crystalline polymer segments (stems) at the outermost positions, and (b) the pinning of a stem at a fixed length because other segments of the stem molecule have been incorporated into the crystal elsewhere. We discuss these effects in more detail below.

The geometry of the lamella is shown schematically in Fig. 1. For simplicity, the stems are shown as being vertical and parallel, and most fold segments connecting various stems are omitted.<sup>10</sup> Any crystal will have a finite degree of surface roughness at finite temperatures, and in our models this is allowed by employing growth units which are not much larger than the molecular repeat unit (e.g., about six  $\text{CH}_2$  groups for polyethylene as in previ-

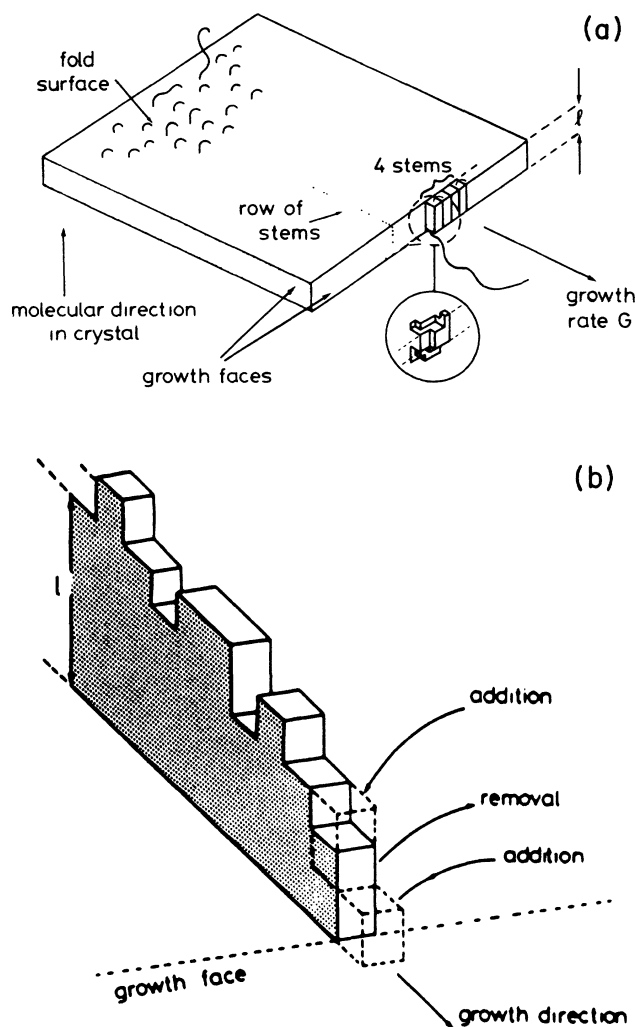


FIG. 1. (a) Representation of a lamellar crystallite, showing stems (chain direction vertical) and a step on the growth face. The inset provides a description of the step in terms of units that are shorter in length than the stem. The dotted lines indicate where the row of stems in (b) is imagined to occur. (b) The basic row of stems model, showing units along the chain as cubes [chain direction vertical as in (a)].

ous theories<sup>2,4</sup>). Such segments of the chain may attach and detach at various points along the growth surface.

Any crystal will have rounded or beveled regions along the edge where two surface planes intersect.<sup>14</sup> In the case of lamellar crystals there may be no significant planar region on the growth faces, since the beveled regions from the top and bottom edges will often merge. Hence, the stem length is expected to decrease on going from the interior of the lamellae toward the growth face. This tapering in the growth region can have a crucial effect on the growth mechanism, as indicated by the following argument.

Constraints are expected to restrict the addition and removal of growth units from the crystal in certain cases. Certainly, once a lamella is formed, it may be difficult to thicken the crystal simply by adding units to the fold sur-

face, since chains from a typical stem will reenter the crystal in other places, and are not available for further extensions of that stem. Even near the growth surface, a coil may attach in several places with taut sections between, and hence create two pinned surface sites.

The combination of the tapered geometry and the pinning of certain sites in this region leads to an entropic barrier. The low-entropy bottleneck corresponds to an improbable configuration in which the growth face is momentarily squared off, so that stems may be incorporated into the bulk which are sufficiently long to provide a thermodynamically stable crystal. The precise way in which pinning is included in the model is not crucial to the behavior of the system. For example, pinning may result from taut loops as discussed above, or simply from the fact that the chain terminates at the site.<sup>8</sup>

The consequences of the entropy barrier for the growth kinetics and thickness selection are similar to those for the nucleation theories of polymer crystallization. If it is assumed that the height of the free energy barrier  $\Delta F$  is simply proportional to  $l$ , then since the growth rate  $G$  depends exponentially on  $\Delta F/kT$ ,

$$G = G_0 \exp(-K_1 l / T_c), \quad (1)$$

where  $K_1$  is a constant and  $T_c$  the temperature during crystallization. Since  $l \propto \Delta T^{-1}$ ,

$$G \approx G_0 \exp(-K_g / T_c \Delta T), \quad (2)$$

where  $K_g$  is a constant. In both models  $G$  varies strongly with  $\Delta T$  mainly because of the  $l$  variation.

Two classes of kinetic model have been outlined: nucleation and pinning on a rough growth surface. In spite of the fundamental difference in the basis of the models, there are strong analogies in the mathematics used to derive the results, i.e., Eqs. (1) and (2). It is particularly useful to note that the growth rate can usually be described by the product of a barrier term, as given above, and a term related to the net thermodynamic driving force. The driving force term is reflected in the value of  $\delta l$ ; when  $\delta l$  is zero the driving growth rate is zero by definition. The models developed by Point<sup>15</sup> and by DiMarzio and Guttman<sup>16</sup> have some similarities with pruning models. They also involve segments of chains shorter than a complete stem.

The extensive data on Poly(ethylene oxide) (PEO) (Ref. 17) provides information on the relationship between  $G$  and  $\Delta T$  without the complications of thickness variations, since  $l$  is largely constrained to values which remain nearly the same for significant regions of  $\Delta T$  (growth branches). Within each branch  $G$  is linear with  $\Delta T$  as expected for a rough-surface growth mechanism,<sup>8</sup> and it varies by factors of 2–4. However, rates for *different* branches vary by factors of 3.5 orders of magnitude. This implies that a barrier term is present which is constant for constant  $l$ .

#### METHODS OF CALCULATION

A simplified two-dimensional row model is used with rate equations to describe transitions to the different possible configurations during growth.<sup>17</sup> Figure 1 shows a

row of stems which grow from the end of the row according to a very simple set of rules: (1) Units can only be added or subtracted from the end of the outermost stem, and underlying stems are pinned at their current length. (2) Initiation or removal of stems is only accomplished by adding a single unit adjacent to the outermost stem, or by removal of the outermost stem when it contains only one unit. The physical basis for these rules has been outlined above. They include the effects of pinning in a form that is relatively tractable to mathematical analysis.

The distribution of stem lengths in an ensemble of row crystals is described by  $C_n(i)$ , the fraction of stems at position  $n$  behind the outermost stem which have a length of  $i$  units. It is also necessary to specify a function which determines the correlations in length of adjacent stems;  $f_n(i, j)$  is the conditional probability that the  $(n+1)$ th stem is of length  $j$  given that the  $n$ th stem is of length  $i$ . Because this represents a one-dimensional array of stems, in the steady-state system  $f_n(i, j)$  is independent of  $n$ . The probability  $P_n(i, j)$  of having stems of length  $i$  at  $n$  and  $j$  at  $n+1$  is then  $f_n(i, j)C_n(i)$ . The rate equations are then designed to include all possible events at position  $n=1$  at the growing face of the crystal; for  $i > 1$ ,

$$\begin{aligned} dP_1(i, j)/dt = & k^+ P_1(i-1, j) \\ & + k^-(i+1, j) P_1(i+1, j) \\ & - k^+ P_1(i, j) - k^-(i, j) P_1(i, j) \\ & + P_1(1, i) k^-(1, i) f(i, j) - k^+ P_1(i, j), \quad (3) \end{aligned}$$

and for  $i=1$ ,

$$\begin{aligned} dP_1(1, j)/dt = & k^+ C_1(j) + k^-(2, j) P_1(2, j) \\ & - k^+ P_1(1, j) - k^-(1, j) P_1(1, j) \\ & + P_1(1, 1) k^-(1, 1) f(1, j) - k^+ P_1(1, j). \quad (4) \end{aligned}$$

Here  $k^+$  is the rate constant for both adding one unit to an existing stem and for the addition of a new stem of unit length adjacent to the outermost stem in the crystal, and  $k^-(i, j)$  is the rate constant for removal of a unit from a stem at  $n=1$  of length  $i$ , when the stem at  $n=2$  is of length  $j$ . The rate constants for removal are

$$k^-(i, j) = k^+ \exp(2\epsilon/kT_M^0 - m\epsilon/kT), \quad (5)$$

where  $m$  is the number of nearest neighbors to the growth unit and  $\epsilon$  is the interaction energy between these units. It is apparent that  $m=2$  when  $i > 1$  and  $j \geq i$ , and  $m=1$  when  $i > 1$  and  $j < i$  or when  $i=1$  and  $j \geq i$ . Situations with isolated growth units ( $m=0$ ) are not permitted according to the rules discussed above. It is only necessary to solve the rate equations for  $n=1$ , Eqs. (3) and (4), since the required information about the stem length distributions beneath can be inferred from the  $f(i, j)$  in the outermost layer.

The 2D row model described above should involve most of the phenomena observed in rough growth surfaces in three dimensions; i.e., for small  $\sigma_n$ . The absence of neighboring growth units in the direction perpendic-

ular to the planar crystal should not change the nature of the results in a fundamental manner. Only in the case of faceted growth fronts is the correlation of growth units along this direction an important factor. Indeed, Monte Carlo simulations of a 2D row model exhibit kinetics similar to those of the three dimensional (3D) model.<sup>17</sup> In particular,  $G$  values obeying Eq. (1) have been obtained, and  $l \propto \Delta T^{-1}$  also gives a good approximation to the calculated thickness values.

#### THE MINIMUM LAMELLAR THICKNESS $l_m$

As noted above, positive growth only occurs when the lamellar thickness  $l$  is greater than  $l_m$ . In fact,  $l_m$  has been assumed to be the value of  $l$  at which  $T_c$  is the melting temperature of the lamella. If a crystal of thickness  $l_m$  were actually in equilibrium with the liquid phase, then  $l_m$  would be determined by equating the free energy of the liquid to that of the lamella, with the result

$$l_m \Delta f = \sigma_e + \sigma'_e, \quad (6)$$

where  $\sigma_e$  and  $\sigma'_e$  are the fold surface-free energies for the upper and lower surfaces, respectively (these are unequal in the row model), and  $\Delta f$  is the bulk free-energy change per growth unit on crystallization. The free-energy change  $\Delta f$  is usually calculated on the assumption that the entropies and enthalpies of the two phases are approximately constant for  $T_c$  in the vicinity of  $T_M^0$ . Thus, the free energy of a single phase is  $F=H-T_c S$ , or  $\Delta f = h - T_c \Delta S$ , where  $h$  is the heat of fusion. Using the fact that  $\Delta f = 0$  at  $T_M^0$ , we have  $\Delta f = h \Delta T / T_M^0$ , and Eq. (6) becomes

$$l_m h \Delta T / T_M^0 = \sigma_e + \sigma'_e \quad (7)$$

for the model with  $\sigma_e \neq \sigma'_e$ , whereas for most polymer systems the surfaces are equivalent and the right-hand side is simply  $2\sigma_e$ . Note that the equation is derived from an approximate expression for the change in free energy on melting, extrapolated from  $T_M^0$ .

In principle, however, this approach is not correct since the crystal of thickness  $l_m$  is not in complete equilibrium at  $T_c$ . Both experiments and the model show that the crystal will thicken at a finite rate. For this reason, a unique definition of  $l_m$  may not be possible. In practice, the issue comes down to the entropy  $S_e$  of the fold surface; i.e., how much does the structure of the fold surface (top surface in Fig. 1) deviate from that of a surface in true equilibrium with the fluid. The lower surface of our model crystal has no disorder, since all stems are constrained to terminate at the same vertical position. Thus,  $\sigma'$  is simply the enthalpy  $\epsilon/2$ . The free energy  $\sigma$  of the upper surface may, under certain conditions, be approximated by the expression for the unrestricted one-dimensional (1D) surface,<sup>18</sup>

$$\sigma_e = \epsilon/2 - kT \ln \left[ \frac{\cosh \epsilon/4kT}{\sinh \epsilon/4kT} \right]. \quad (8)$$

The surface enthalpy includes broken bonds in the hor-

horizontal and vertical directions, and is given by

$$h_e = \epsilon/2 + \epsilon/(2 \sinh \epsilon/2kT). \quad (9)$$

In order to study a system where  $l_m$  and  $\delta l$  are unambiguous quantities, we employed a large value of  $\epsilon$ ,  $5kT$ , where the surface disorder on the upper surface is small and  $\sigma_e \approx \epsilon/2$ . The validity of these results for smaller  $\epsilon$  was tested by the following procedure: (i) Measure  $l$  on a system in which certain thicknesses are energetically preferred. (This can be accomplished experimentally by the use of monodisperse short chain materials such as PEO.) In this particular row model the fold surface structure can be measured for nonequilibrium conditions without changes in the thickness of the crystal, because the metastable system "locks in" to one preferred thickness. If these results indicate that the nonequilibrium structure deviates only a small amount from that for equilibrium conditions, then Eqs. (8) and (9) can be used to describe the surface. (ii) A second approach is to impose a constraint limiting the stem length to a specified maximum value. That is, transitions to stems longer than this value are excluded from Eqs. (3) and (4). Then a condition of zero growth can be achieved for  $T < T_M^0$  by trial and error. The fold surface will not be equivalent to the unrestricted surface because the constraint limits the disorder and reduces  $S_e$ . For this reason this procedure yields an upper limit to  $\sigma_e$ .

#### CRYSTAL GROWTH AT A SPECIFIED THICKNESS

As discussed above, a model that has preferred values of the lamellar thickness  $l$  has direct applications to low molecular weight polymers, PEO in particular, and also should provide new information on the relationship between  $G$  and  $\Delta T$ .

Certain stem lengths are selected by modifying the energy of some configurations in such a way as to stabilize the selected value or to destabilize others.<sup>8</sup> Changes are effected only for two adjacent stems of the same length. If this length is equal to the desired thickness  $l_p$ , the energy is reduced by an amount  $\delta\epsilon$ , and for other pairs of equal length it is increased by  $\delta\epsilon$ . The rate constants are modified accordingly;

$$k'(i,i) = \begin{cases} k^-(i,i)\exp(-\delta\epsilon/kT), & i = l_p \\ k^-(i,i)\exp(\delta\epsilon/kT), & i \neq l_p \end{cases} \quad (10)$$

If only one  $l_p$  is specified, the value of  $l$  calculated is constant with  $T_c$  for  $\delta\epsilon > 0.7kT$ . Figure 2 shows some of the growth rates plotted versus  $T_c$ . The linear dependence of  $G$  versus  $\Delta T$  found for simulations<sup>8</sup> and experiments on PEO (Ref. 18) can clearly be seen in the results from this model also. At the higher values of  $l$  the plots show an increasing degree of curvature.

The results on surface energies have applications to the problem of calculating  $\delta l$  when  $\delta\epsilon = 0$ . Figure 3 shows values of the number of broken horizontal bonds in the upper fold surface for one of the growth branches. This number is a measure of the surface energy  $h_e$ . The surface energy for  $G = 0$  corresponds to equilibrium. As  $G$  increases, one might expect large departures from the

equilibrium value. However, Fig. 3 shows that this is not the case. Thus we see that the surface energy corresponds closely to the equilibrium value even when there is a net accumulation rate of material on the crystal. Because of this it should be possible to define a value of  $\sigma_e$  using the equilibrium  $S_e$ , except perhaps in the limit of

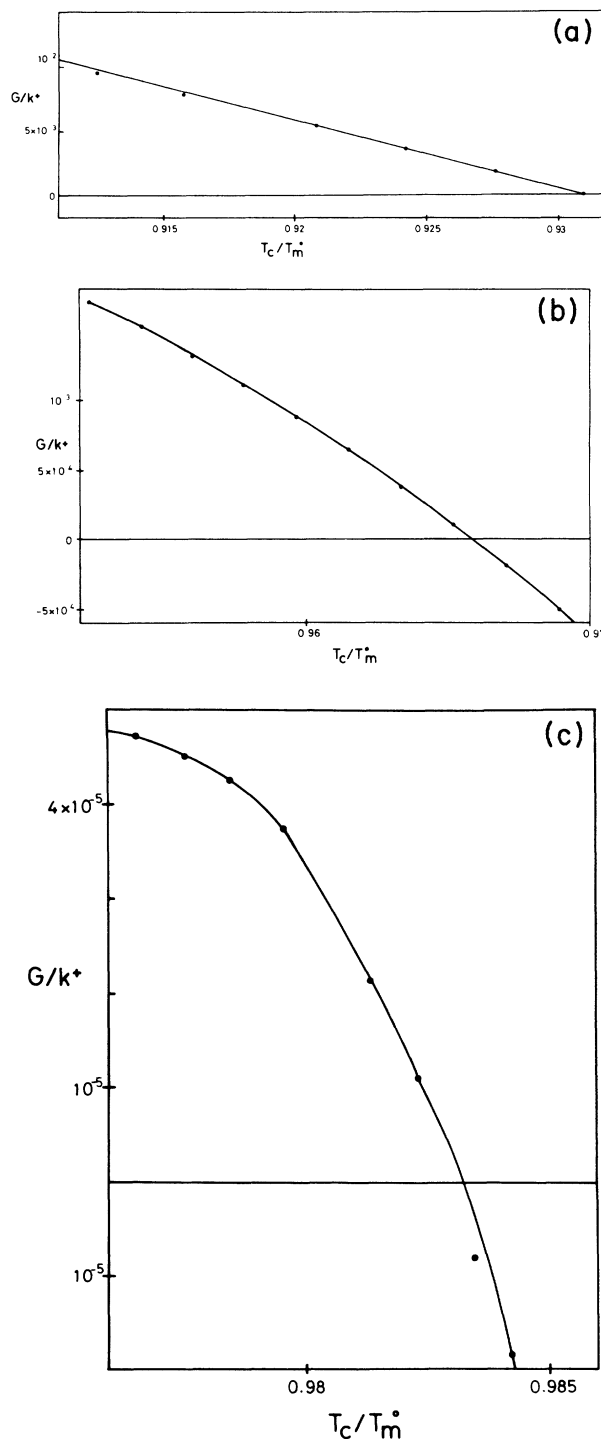


FIG. 2. Growth rate  $G$  vs  $\Delta T$  for the system where a preferred  $l$  value has been imposed; for  $\delta\epsilon = 0.7kT_m^0$ , (a)  $l = 4$ ; (b)  $l = 8$ ; and (c)  $l = 12$  chain units:  $kT_m^0/\epsilon = 0.55$ .

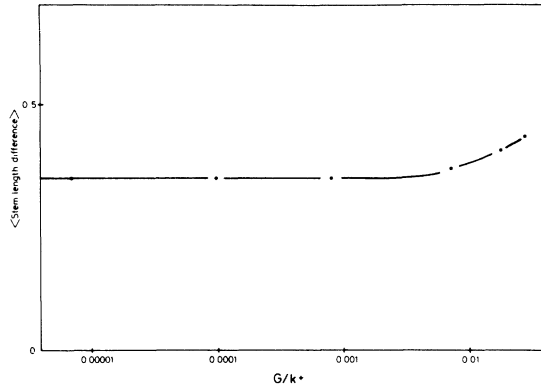


FIG. 3. Values for the density of lateral "broken bonds" in the completed crystal. The surface energy includes that associated with these changes in stem lengths (leading to steps on the "top" surface) and additional contributions from  $\delta\epsilon$ :  $l_p=4$ ,  $\delta\epsilon=\pm 0.7kT_m^0$ ,  $kT_m^0/\epsilon=0.55$ . The different growth rates  $G$  on the abscissa were obtained from changes in  $\Delta T$ .

very large growth rates. The  $h_e$  values given in Fig. 2 do not correspond to Eq. (9) since the additional energy contributions  $\delta\epsilon$  are present.

## RESULTS FOR UNRESTRICTED STEM LENGTHS

### Small fold surface disorder ( $\epsilon=5kT$ )

Calculated values of  $l$  are plotted as a function of  $T$  in Fig. 4(c), together with  $l_m$  from Eqs. (6) and (8). It can be seen that  $\delta l$  is approximately 0.7 of the length of a growth unit over most of the temperature range. The average length of a stem as a function of the position behind the growth face is shown in Fig. 5, and the distributions of  $C_1$  are shown in Fig. 6. It can be seen that the rounding or beveling is relatively small for this value of  $\epsilon$ . There is still a finite entropy barrier to achieving the squared profile, however, and this is apparent in the growth rate data. The probability of finding a stem at the end equal in length to the average  $l$  of the lamella can be measured directly from the numerical data; it is given by  $C_1(l)$ . The relationship between the growth rate and  $C_1(l)$  will be given below in a discussion of the factors that determine  $\delta l$ .

### Significant fold surface disorder

A more general case for polymers is that in which the fold surface contains large numbers of exposed sides of stems. From the previous results it can be expected that  $\sigma_e$ ,  $h_e$ , and  $S_e$  are close to their equilibrium values. This was checked by calculating  $h_e$  from the values of  $P(i, j)$ . It was found that these agree closely with those predicted from Eq. (9), even in the case of high surface disorder ( $\epsilon=1.82kT$ ). We conclude that the effect of the growth process on the disorder in the top surface is small for the range of growth rates of interest.

One further check was made of the  $l_m$  results by restricting the maximum value  $i$  of the stem length, and

then adjusting the temperature to give zero growth. This procedure gives very accurate agreement with  $l_m$  calculated from Eq. (6) for large  $\epsilon$ . However, when even a small amount of disorder is present in the fold surface, the restriction on  $i$  does reduce the disorder and this is seen from the reduced  $h_e$  values. The restricted surface has a higher value of  $\sigma_e$  than the unrestricted one, since the constraint excludes configurations that might otherwise appear in an equilibrium ensemble. The restricted system should provide an upper limit to  $l_m$ . These results are entered in the plots in Fig. 4 as vertical lines with a bar to indicate the upper limit on  $l_m$ .

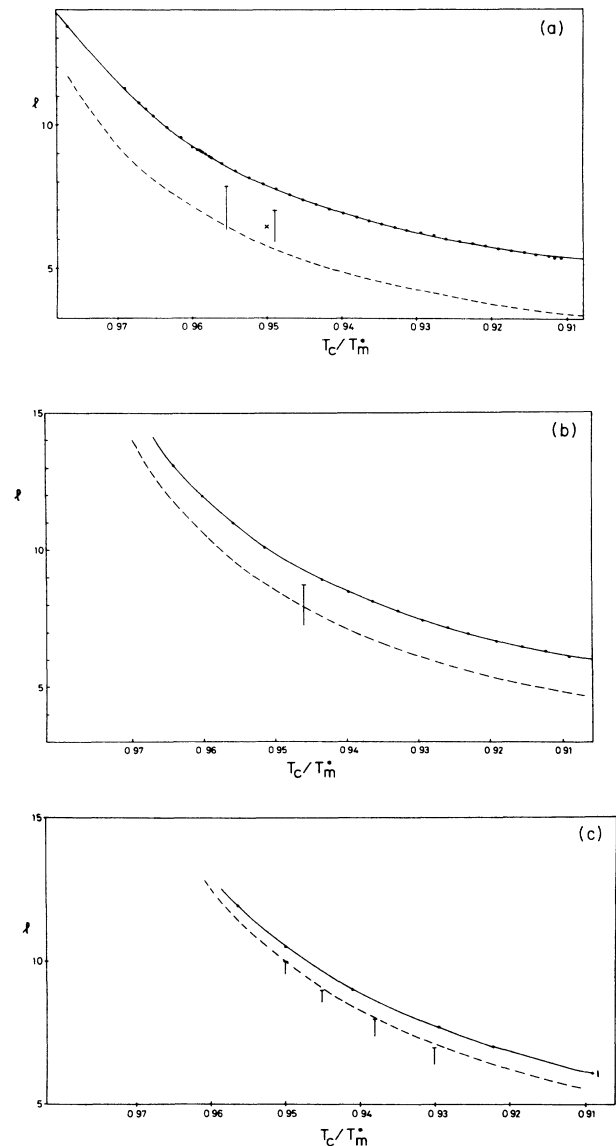


FIG. 4. Plots of  $l$  and  $l_m$ : estimates for three values of  $\epsilon$  [(a)  $kT_m^0/\epsilon=0.55$ ; (b)  $kT_m^0/\epsilon=0.35$ , and (c)  $kT_m^0/\epsilon=0.2$ ]. The dashed lines refer to estimates of  $l_m$  from Eq. (6), the bars to upper limits on  $l_m$  from data on crystals constrained to limited stem length, and the crosses to values  $l_m$  obtained by extrapolating the driving force term to zero.

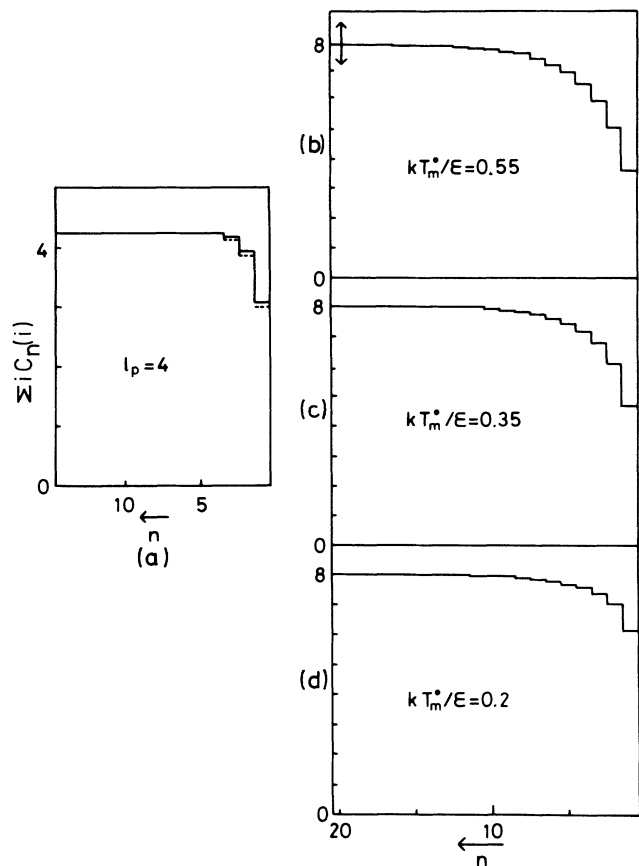


FIG. 5. Properties of the growth front of the crystals: the average length of the stems for a range of  $n$  for  $20 \geq n \geq 1$  is plotted. The vertical arrows in (b) indicate the root-mean-square magnitude of the fluctuations in stem lengths.

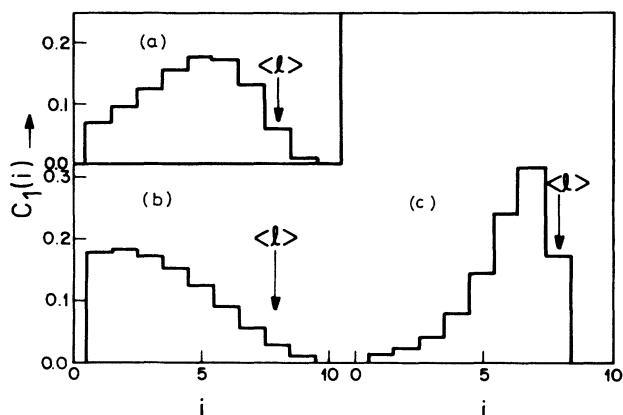


FIG. 6. Histograms of  $C_1(i)$  for  $\langle l \rangle \sim 8$  for (a)  $kT_m^0/\epsilon = 0.55$ ; (b)  $kT_m^0/\epsilon = 0.35$ ; (c)  $kT_m^0/\epsilon = 0.2$ . The values of  $\langle l \rangle$  calculated from  $C_{20}(i)$  are indicated by arrows. The values of  $C_1(i)$  beyond the peaks in the distribution is replotted in Fig. 7(b).

The results for disordered fold surfaces show that  $\delta l$  is about 1.2 units in length for  $\epsilon = 1.82kT$ , significantly larger than the value obtained for  $\epsilon = 5kT$ . Values of  $\delta l$  can be inferred from Fig. 4. The data for  $\epsilon = 1.82kT$  correspond to a small value of  $\sigma_e$ , such that  $\sigma_e \ll \epsilon/2$ . This system is close to the 2D critical temperature where the interface energy vanishes altogether.<sup>19</sup> This situation is probably not relevant to most polymer crystals, and the data plotted for the intermediate value of  $\epsilon = 2.86kT$  shown Fig. 4(b) are more realistic.

#### IDENTIFICATION OF PHYSICAL PROCESSES FROM THE GROWTH EQUATION

We now return to the description of any kinetic theory of lamellar growth rates in terms of a product of a barrier term  $a_0(l)$  and a driving force term  $d(\delta l)$  (see also Ref. 4):

$$G = k + a_0(l)d(\delta l). \quad (11)$$

The term  $a_0(l)$  generally has an exponential dependence on  $l$ , describing the probability of surmounting the barrier, whereas the driving force term  $d(\delta l)$  is approximately linear in  $\delta l$ . For example, the simplest expression describing nucleation theory given by Frank and Tosi<sup>2</sup> is

$$G_{\text{nucl}} = A_0(1 - B/A). \quad (12)$$

Here  $A_0$  is given by  $\beta \exp(-2\sigma_n/kT)$ , where  $\beta$  represents an incident flux of complete stems and where  $\sigma_n$  is assumed to increase linearly with  $l$ . The factor  $B/A$  is the ratio of removal to addition rates for stems at niche sites. The term in brackets goes to zero at equilibrium, where  $B = A$ , and increases proportionately with  $\delta l$  for small  $\delta l$ .

We have identified the *barrier term* in the row model as the probability  $C_1(l)$  of finding a rectangular growth face. An interesting question in this approach is whether there is a local equilibrium such that equilibrium thermodynamics could be used to calculate the barrier term  $C_1(l)$ . [For nucleation theories, this is implicit in the use of Boltzmann expressions such as  $\exp(-2\sigma_m/kT)$ .] The results with specified crystal thickness (Figs. 2 and 3) suggest that there is approximate equilibrium in the row model. Further work pursues the question of calculating  $a_0(l)$  on the basis of equilibrium.<sup>19</sup> However, significant deviations from equilibrium can occur in the row model when  $\epsilon$  values are different along and between stems.<sup>20</sup> These produce interesting effects in the growth rate behavior.

The simplest assumption for the driving force term  $d(\delta l)$  would be equivalent to the formula for condensation of liquid on to a liquid surface:

$$d(\delta l) = 1 - \exp(-\delta f/kT), \quad (13)$$

where  $\delta f$  is the free-energy driving force, which is related to  $\delta l$  by the relation

$$\delta f = \Delta f - (\sigma_e + \sigma_e')/l = h\Delta T\delta l/(lT_m^0). \quad (14)$$

In view of Eqs. (11)–(13), it is useful to rewrite the equation for  $G$  for the row model as follows. Consider

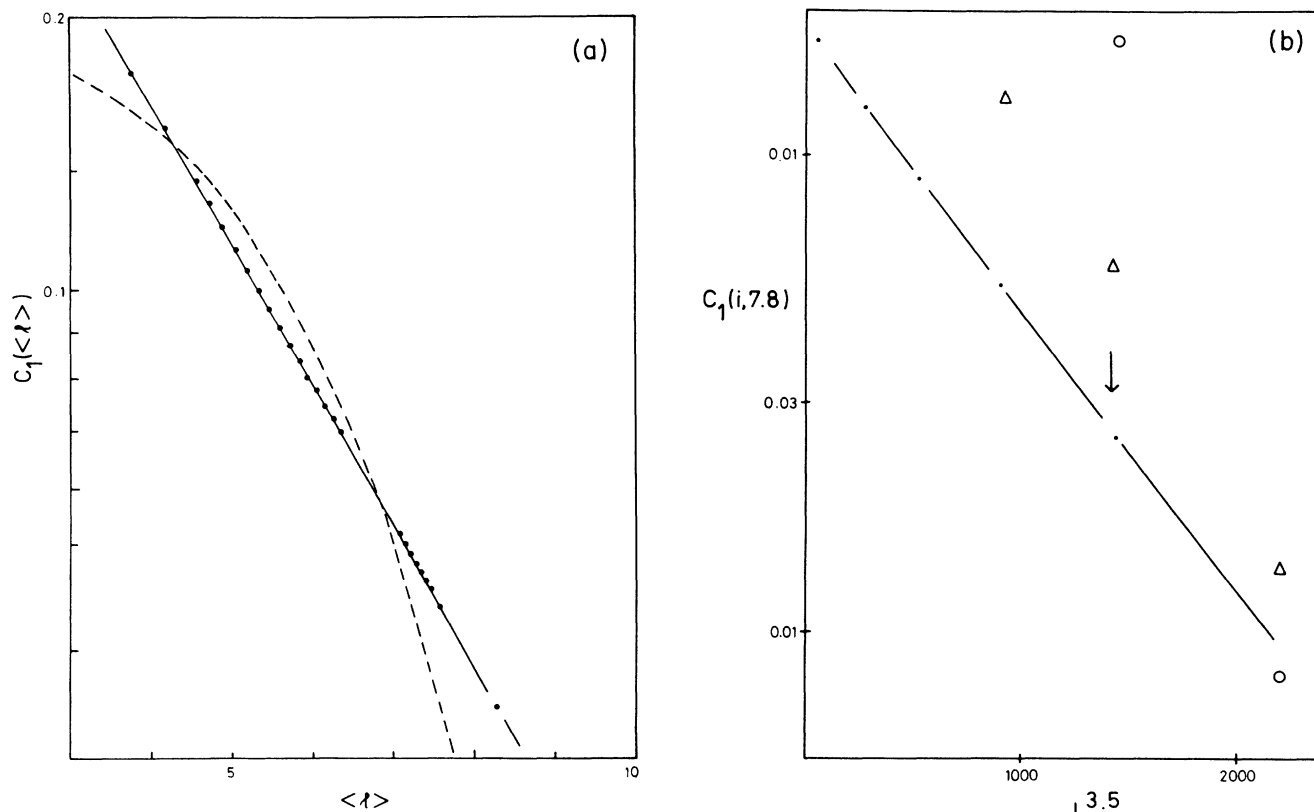


FIG. 7. (a) Values of  $C_1(\langle l \rangle)$  vs the average  $\langle l \rangle$  at  $n = 20$  values, i.e., crystals grown at different values of  $\Delta T$ ;  $kT_m^0/\epsilon = 0.55$ . In order to allow for nonintegral values of  $\langle l \rangle$ , the  $C_1(\langle l \rangle)$  were calculated with weighting factors  $C_{20}(k)$ , i.e., the stem length distribution sufficiently far behind the growth front to approximate the bulk of the crystal. The dashed line corresponds to the dependence of  $C_1(i)$  as a function of  $i$  for  $\langle l \rangle = 8$ . This quantity is also shown in (b). The 3.5 power is required for a linear plot and indicates the more rapid decrease in  $C_1(i)$  in the self-consistent barrier calculation:  $kT_m^0/\epsilon = 0.55$ .

the net deposition rate of stems of a specified length  $i$ . The fraction of the total growth rate corresponding to the deposition of these stems is

$$G(i) = k^+ C_1(i) - k^-(1, i) P_1(1, i). \quad (15)$$

This follows, since the stems of length  $i$  must be covered by a new stem of length 1 to be incorporated into the crystal. This equation can be written as

$$G(i) = k^+ C_1(i) \{ 1 - [k^-(1, i)/k^+] P_1(1, i)/C_1(i) \}. \quad (16)$$

The term  $C_1(i)$  multiplying the brackets can be regarded as the barrier, since it represents the probability of finding the system in the transition state, and this may not be much affected by the kinetics. The term in curly brackets is closely related to the free-energy driving force for crystallization [see Eq. (13) for example].

Plots of  $a_0$  are shown in Fig. 7(a), and the term in square brackets is shown in Fig. 8. The curve for  $a_0(l)$  was calculated from the  $C$  values as follows. A series of  $\Delta T$  values were specified; the average thickness in the body of the crystal ( $l$ ) and the  $C_1(i)$  were found. Then  $a_0$  was calculated from a weighted average of  $C_1(i)$ , using the distribution of stem lengths in the body of the crystal; this was approximated by  $C_{20}(i)$ , since the distribution

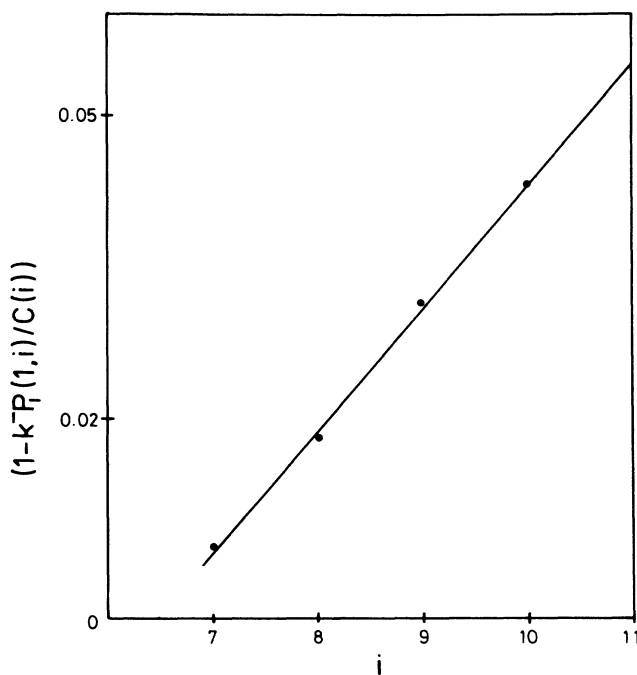


FIG. 8. The driving force factor  $d(i)$  as derived from the  $P_1(i, j)$  as obtained using Eqs. (11) and (16) ( $kT_m^0/\epsilon = 0.55$  as in Fig. 7).

was found to remain essentially unchanged for stems farther than 20 units back from the growth front. Thus, the value of  $a_0$  represents the probability of finding at position  $l$  a stem of the correct length to satisfy the bulk distribution of stem lengths. The  $C$  values were obtained from the  $P(i, j)$  values in the numerical solution of the rate equations. Figure 7(a) shows that the relationship of  $C_1$  to  $l$  is approximately exponential, as in the nucleation models of polymer crystallization, according to

$$a_0(l) \propto \exp(-\kappa l), \quad (17)$$

where  $\kappa = 0.35$  for  $\epsilon = kT_m^0/0.55$ . Figure 8 shows a linear dependence of the driving force term  $d(i)$  on  $i$  for one value of  $L$ . The intercept on the  $l$  axis in Fig. 8 produced by extrapolation gives an estimate of  $l_m$ , since  $l_m$  is defined as the value of  $l$  where the driving force vanishes. The slope of the curve in Fig. 8 is considerably less than that assumed in Eq. (13), and this effect will be discussed elsewhere.

#### METHODS OF CALCULATING $\delta l$ USING THE CRITERION OF FASTEST GROWTH

In this section we apply the interpretation of the growth mechanism given in the preceding section. We wish to examine the analogue of the argument given by Frank and Tosi in describing the nucleation model.<sup>2</sup> That is, in an ensemble of crystals, those which dominate the statistics are the ones with the most material, or those with the fastest rate of growth. Thus, the expected thickness  $l$  is the value which maximizes the product of the two terms discussed above. Figure 9 shows  $A_0(l)$  and the driving force expression for the nucleation model, using accepted values for the parameters normally used,<sup>3</sup> and shows the maximum in  $G$  (dashed line, compare with Fig. 1 of Ref. 2). In either type of kinetic model, nucleation or pinning, there are two approaches that can be used for the calculation of  $l$ .

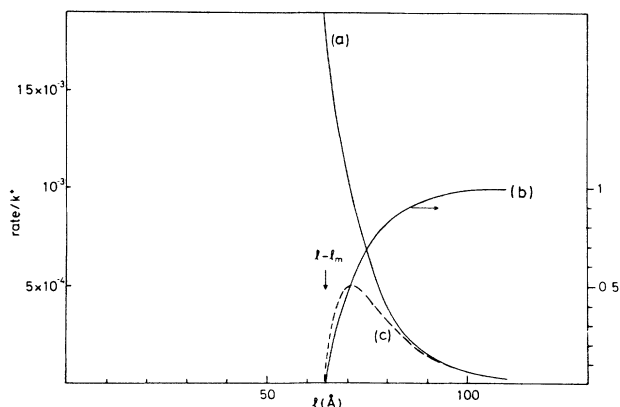


FIG. 9. Growth rate, as calculated for the nucleation model, for one value of  $i$ , i.e., the overall incorporation rate for stems of length  $i$ . Also shown are the contributing factors from the barrier and from the driving force. (a) Barrier term  $A_0$ ; (b) driving force term is  $(1-B/A)$  [see Eq. (12)]; (c) total initiation rate for new patches on the growth face which under some conditions gives the growth rate  $G$ .

At the one extreme, as envisioned by Lauritzen and Hoffman,<sup>1</sup> there is an ensemble of crystals with a range of thicknesses, but each crystal is assumed to have a uniform thickness  $l$ . The observed thickness is assumed to be equal to the ensemble average. The equivalent for the row model is to take the product of  $a_0(l)$ , Eq. (17), and  $l - l_m$ , which is proportional to the driving force factor, and differentiate in order to find the maximum in  $G$ . The result is  $\delta l = 3.3$ , which is clearly too high compared with the actual data shown in Fig. 4.

It is also clear that the assumption of uniform thickness along the length of the model crystal could have an important influence on the results. Fluctuations are explicitly eliminated by the assumption of constant thickness. In the present model,  $f(i, j)$  for  $i \neq j$  is significant, showing that thickness changes do occur. Similarly, experiments<sup>15,21</sup> have shown that changes in the temperature during crystallization cause thickness changes such that the crystal adjusts its thickness to suit the new conditions. A surface step is produced at the position where the growth front was located when the conditions were changed.

Frank and Tosi<sup>2</sup> first recognized this deficiency in the context of the nucleation model, and in their theory the stems in a crystal are permitted to have different lengths. The crystal evolves in a self-consistent manner to produce an average stem length or thickness  $l^{**}$ . The theory predicts that, within a single crystal, stems longer than  $l^{**}$  are disfavored, because they are likely to require overhangs with high surface energies.

A similar self-consistent approach can be used to describe the pinning models. Consider an ensemble of growing crystals with an average thickness  $l$ . Let  $C_1(i)$  be the concentration of the subset consisting of crystals that have a stem at the outermost position of length  $i$ . Figure 7(b) shows that this decreases faster with increasing  $i$  than does  $a_0(l)$  in Fig. 7(a). Note that Fig. 7(b) derives from one set only of  $P(i, j)$  values corresponding to a single  $\Delta T$ . This is not true for Fig. 7(a). It was found by trial and error that for  $\epsilon = kT_m^0/0.55$   $C_1(i)$  depends on  $i$  according to the relation

$$C_1(i) = \exp[-(i/l_0)^\gamma], \quad (18)$$

where  $\gamma$  is about 3.5 and  $l_0 = 6.6$ .

By the use of Eq. (18) for  $C_1(i)$ , we can calculate  $l$  from the maximum of the product of this with the driving force term in Eq. (16) (curly braces) which has been described in Fig. 8. Figure 10 shows  $C_1(i)$  and the driving force expression for the row models, and the sharp maximum in  $G$  can be observed in the product (dashed line). An approximate value for  $l$  should be given by the value that maximizes the quantity  $[(l - l_m)/l] \exp[-(l/l_0)^\gamma]$ . Note that the thickness  $l$  will not be affected by a change in the constant multiplying the expression for the driving force. The condition for  $l$  is then

$$\gamma l^{\gamma+1} - \gamma l_m l^\gamma - l^\gamma l_M = 0. \quad (19)$$

The value of  $l$  is close to the measured value in most cases, where the model calculations were made; typical results are  $l = 7.6$  for (19) and  $l = 7.9$  for the model. A



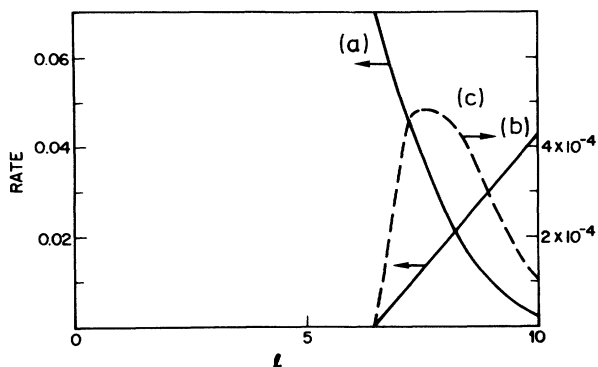


FIG. 10. As in Fig. 9, but showing analogous results for the row of stems model, taken from Figs. 7 and 8: (a) barrier term from Fig. 7(b); (b) driving force term from Fig. 8; (c) total growth rate as the product of (a) and (b) showing the preferred  $\langle l \rangle$  value.

more precise way of calculating the average  $l$  is to average under the dashed line in Fig. 10. This is in fact equivalent to the derivation of a growth kinetics from the rate equations. The purpose of using Eq. (19) is not in fact to derive precise  $l$  values but rather to see if the physical processes operative in the row model are consistent with the description of a kinetic model in terms of maximizing  $G$ . Our conclusion is that the self-consistent approach should be used to allow for fluctuations in thickness, and in this case the method gives results in agreement with the model.

### GROWTH RATES

The plots of  $G$  in Fig. 11 are not strictly linear, in contrast with the highly linear plot of  $a_0(l)$  on a log scale against  $l$  [Fig. 7(a)]. This reflects the fact that  $l$  is not

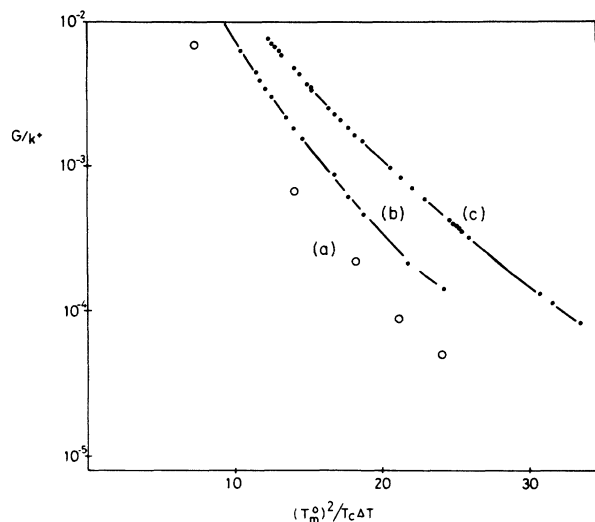


FIG. 11. Logarithmic plot of the growth rate  $G$  for the row model vs  $(T_m^0)^2/T_c \Delta T$ , according to Eq. (12) as expected for nucleation theory. As is explained in the text, Eq. (12) can represent growth limits by any activated state, such that the activation energy depends on  $\Delta T^{-1}$ . Here (a) corresponds to  $kT_m^0/\epsilon=0.2$ , (b)  $kT_m^0/\epsilon=0.35$ , and (c)  $kT_m^0/\epsilon=0.55$ .

very accurately proportional to  $\Delta T^{-1}$  as assumed in Eq. (2). Nucleation theories usually associated nonlinear growth kinetics with regime changes. The 3D models<sup>11</sup> show both linear and convex growth plots, so there appears to be scope for a pinning model to account for the different types of kinetics observed experimentally. It is apparent from Fig. 11 that the  $G$  versus  $\Delta T$  relation is similar for the different values of  $\epsilon$ , but the absolute values of  $G$  are lower for large  $\epsilon$ . On the other hand, the results illustrated in Fig. 6 show that this is not a result of smaller values of  $C_1(l)$  at large  $\epsilon$ . In fact, the driving force term is considerably smaller for the larger  $\epsilon$ . There appear to be at least two effects involved here. Firstly,  $\delta l$  is smaller which of course decreases  $d(\delta l)$  (Fig. 4). This explains the large difference between the results for  $\epsilon/kT=1.82$  and  $\epsilon/kT=5$ . Secondly, the probability of finding a short stem at the outermost position is small, and this decreases with increasing  $\epsilon$ . This is a result of the fact that single units, for example, are weakly bonded to the underlying crystal. The state with a singly attached unit may have a smaller probability of appearing in the ensemble than the state with the rectangular growth front.

### DISCUSSION AND SUMMARY

The rate equation approach has shown that the pinning model can account for the principal experimental trends for crystal thickness and growth rate, without invoking nucleation. Many of the results mirror those of the nucleation theories, and in view of the mathematical analogies this is not surprising. For example,  $\delta l$  is approximately constant with  $l$ , and for a typical value of  $l$  it represents about 10% of the total. In this paper we have attempted to identify the physical processes in the row model that determine these results, in particular, we have been concerned with the thickness deviation  $\delta l$ . Our approach has been to separate the expression for the growth rate into two terms. One term represents the probability of finding a crystal in the "transition state," i.e., a crystal with a rectangular end, since only these crystals are available for the addition of a viable stem. The second term represents the rate of deposition on these crystals, and is roughly proportional to the free-energy driving force for crystal growth. This separation is justified by an examination of the properties of the model calculated from the solution of the rate equations. In particular, the barrier term is found to depend exponentially on the average stem length  $l$  and the driving force term is proportional to  $\delta l$  (it goes towards a value near the expected value of  $l_m$ ). The criterion of a kinetic theory, that the small crystal thickness  $l$  is the outcome of the fastest mode of growth, is fully consistent with the results. However, the choice of the appropriate barrier factor is quite a delicate matter. This question may be further illustrated by a discussion of why  $\delta l$  decreases with increasing  $\epsilon$ . The  $a_0(l)$  values decrease more slowly with  $l$  for high  $\epsilon$  compared with low  $\epsilon$ . This is a result of the fact that it is always likely for a fluctuation to decrease  $l$  values compared with the substrate. It is then unlikely, for large  $\epsilon$  especially, for a fluctuation to restore the larger  $l$  values. This is be-

cause of the energy penalty associated with a stem projecting above the substrate. Hence the appropriate barrier factor to discuss is  $C_1(i)$  [Fig. 7(b)]. The  $C_1(i)$  values for one given row crystal decrease more steeply with  $i$  for the case of larger  $\epsilon$ . Hence, once rows are established, there is a decreased probability of maintaining a large  $\delta l$  for the case of large  $\epsilon$ .

The differences in properties for different  $\epsilon$  are intriguing and have no counterpart in nucleation theories. The side surface free-energy term  $\sigma$  in nucleation theories is

affected by the strength of the intermolecular bonding, but it is usually considered to be a constant for a given geometry. It influences the  $K_g$  values through the barrier term for step creation. To a first approximation,  $\epsilon$  does not change the barrier term for the row model, but scales the growth rates as a whole. This may be relevant to the striking experimental observation<sup>22</sup> that growth rates increase rapidly with  $T_c$ , for a fixed  $\Delta T$ . This is accomplished experimentally by the use of different solvents which change  $T_M^0$ .

- 
- <sup>1</sup>J. I. Lauritzen and J. D. Hoffman, *J. Res. Nat. Bur. Stand.* **64A**, 73 (1960).
- <sup>2</sup>F. C. Frank and M. Tosi, *Proc. R. Soc. London, Ser. A* **263A**, 323 (1961).
- <sup>3</sup>J. D. Hoffman, G. T. Davis, and J. I. Lauritzen, in *Treatise on Solid State Chemistry*, edited by N. B. Hannay (Plenum, New York, 1976), Vol. 3, Chap. 7.
- <sup>4</sup>J. J. Point, *Macromolecules* **12**, 770 (1979).
- <sup>5</sup>J. D. Hoffman, *Polymer* **24**, 3 (1983).
- <sup>6</sup>D. M. Sadler, *Polymer* **24**, 1401 (1983).
- <sup>7</sup>D. M. Sadler, *Polym. Commun.* **25**, 196 (1984).
- <sup>8</sup>D. M. Sadler, *J. Polym. Sci. Phys. Ed.* **23**, 1533 (1985).
- <sup>9</sup>D. M. Sadler, M. Barber, G. Lark, and M. J. Hill, *Polymer*, **27**, 25 (1986); B. Wunderlich, in *Macromolecular Physics* (Academic, New York, 1983), Vol. I.
- <sup>10</sup>D. M. Sadler, *Polymer Commun.* **27**, 140 (1986).
- <sup>11</sup>D. M. Sadler and G. H. Gilmer, *Polymer* **25**, 1446 (1984).
- <sup>12</sup>A. Keller, *Philos. Mag.* **2**, 1171 (1957).
- <sup>13</sup>B. Wunderlich, in *Macromolecular Physics* (Academic, New York, 1983).
- <sup>14</sup>C. Herring, *Phys. Rev.* **82**, 87 (1951).
- <sup>15</sup>J. J. Point, C. M. Colet and M. Dosière, *J. Polym. Sci. Phys. Ed.* **24**, 357 (1986).
- <sup>16</sup>E. A. DiMarzio and C. M. Guttman, *J. Appl. Phys.* **53**, 6581 (1982).
- <sup>17</sup>D. M. Sadler and G. H. Gilmer, *Phys. Rev. Lett.* **56**, 2708 (1986); D. M. Sadler, in *Structure of Crystalline Polymers*, edited by I. Hall (Applied Science, 1984), p. 125.
- <sup>18</sup>C. P. Buckley and A. J. Kovacs, in *Structure of Crystalline Polymers*, edited by I. Hall (Applied Science, City, 1984).
- <sup>19</sup>H. J. Leamy, G. H. Gilmer, and K. A. Jackson, in *Surface Physics of Materials*, edited by J. M. Blakeley (Academic, New York, 1975), Vol. I; D. M. Sadler, M. Barber, G. Lark, and M. J. Hill, *Polymer*, **27**, 25 (1986).
- <sup>20</sup>D. M. Sadler, *Nature* **326**, 174 (1987).
- <sup>21</sup>D. C. Bassett and A. Keller, *Philos. Mag.* **7**, 1553 (1962).
- <sup>22</sup>S. Organ and A. Keller, *J. Polym. Sci. Phys. Ed.* **24**, 2319 (1986).

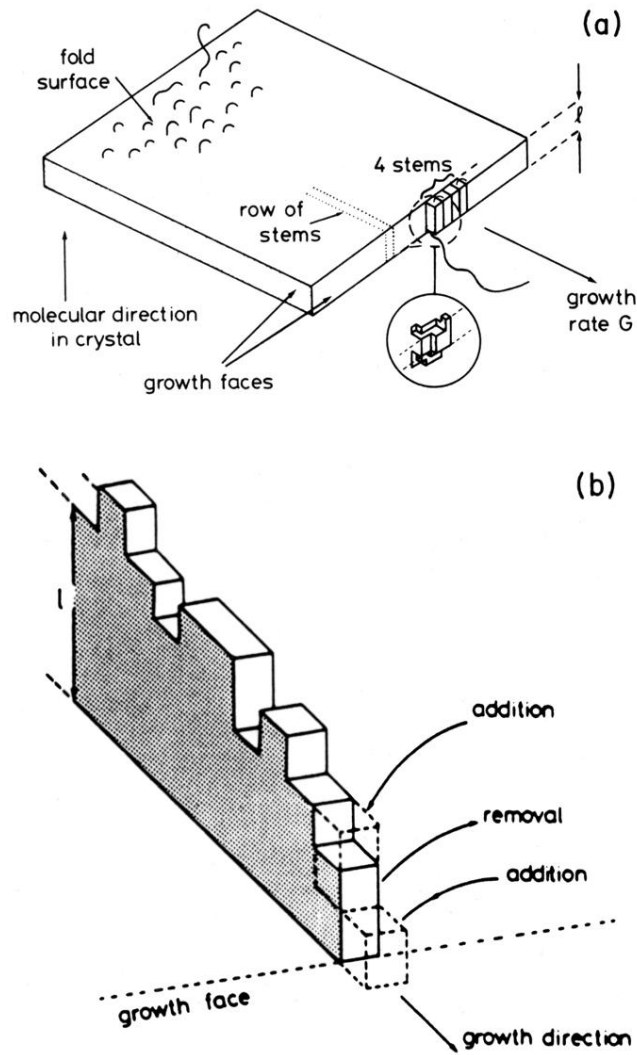


FIG. 1. (a) Representation of a lamellar crystallite, showing stems (chain direction vertical) and a step on the growth face. The inset provides a description of the step in terms of units that are shorter in length than the stem. The dotted lines indicate where the row of stems in (b) is imagined to occur. (b) The basic row of stems model, showing units along the chain as cubes [chain direction vertical as in (a)].